



This open access document is published as a preprint in the Beilstein Archives with doi: 10.3762/bxiv.2019.82.v1 and is considered to be an early communication for feedback before peer review. Before citing this document, please check if a final, peer-reviewed version has been published in the Beilstein Journal of Nanotechnology.

This document is not formatted, has not undergone copyediting or typesetting, and may contain errors, unsubstantiated scientific claims or preliminary data.

Preprint Title Solution-processible Cd-doped ZnO nanoparticles as an electron transport layer to achieve high performance polymer solar cells through improve conductivity and light transmittance

Authors Jianfeng Li, Meiling Ren, Jicheng Qing, Yufei Wang, Zezhou Liang, Ningning Wang, Junfeng Tong, Chunyan Yang and Yangjun Xia

Publication Date 05 Aug 2019

Article Type Full Research Paper

ORCID® iDs Jianfeng Li - <https://orcid.org/0000-0002-1361-4381>

License and Terms: This document is copyright 2019 the Author(s); licensee Beilstein-Institut.

This is an open access publication under the terms of the Creative Commons Attribution License (<http://creativecommons.org/licenses/by/4.0>). Please note that the reuse, redistribution and reproduction in particular requires that the author(s) and source are credited.

The license is subject to the Beilstein Archives terms and conditions: <https://www.beilstein-archives.org/xiv/terms>.

The definitive version of this work can be found at: doi: <https://doi.org/10.3762/bxiv.2019.82.v1>

Solution-processible Cd-doped ZnO nanoparticles as an electron transport layer to achieve high performance polymer solar cells through improve conductivity and light transmittance

Jianfeng Li*, Meiling Ren, Jicheng Qing, Yufei Wang, Zezhou Liang, Ningning Wang, Junfeng Tong, Chunyan Yang, Yangjun Xia*

School of Materials Science and Engineering, Lanzhou Jiaotong University, Lanzhou, 730070, PR China.

Jianfeng Li, E-mail: ljfpyc@163.com(J.Li)

Yangjun Xia, E-mail: xiayangjun2015@126.com(Y.Xia)

Abstract: In this work, electron transport layers (ETLs) with high charge transfer ability was fabricated by doping ZnO nanoparticles with different concentrations of cadmium. The performance for an inverted polymer solar cell based on PTB7-Th: PC₇₁BM with 5% cadmium doping of zinc oxide nanoparticles (CZO) ETL is better than pure ZnO, which can enhance the short-circuit current (J_{sc}), from 16.30 mA/cm² to 17.15 mA/cm², the fill factor (FF) from 64.45% to 69.38%, power conversion efficiency (PCE) from 8.09% to 9.28%. Its consequence of performance stems from curbing interfacial charge recombination and effective charge extraction. Meanwhile, Taking a series of characterization methods, such as atomic force microscopy (AFM), the space charge limited current (SCLC), transmittance, the charge dissociation probabilities ($P(E,T)$), photo-electrochemical impedance spectroscopy (EIS). The results indicate that the electrical conductivity and transmittance of the films are improved by incorporation of Cd in the ZnO film, restrained surface charge recombination and enhanced the electron-transport capability. Therefore, the ETL of Cd-doped will be an ideal candidate for future optoelectronic devices.

Keywords: inverted polymer solar cells; ZnO nanoparticles; cadmium doping; transmittance, electrical conductivity

1. Introduction

Polymer solar cells (PSCs) have gained a lot of attention in the last few decades

because of its solution processable, inexpensive and convenience and extensive roll-to-roll manufacturing [1-10]. Most of them are developing rapidly, with PCE exceeding 14% of single solar cells [11], and of 17% with tandem PSCs [12]. There are two main types of PSCs: conventional and inverted structures. Numbers of conventional structures, poly(3,4-ethylenedioxiophene):poly-(styrenesulfonate) (PEDOT:PSS) as a kind of hole transport layer (HTL) to gather holes, the cathode of a low work-function metal just like aluminum (Al) as electron transport layer (ETL) to collect electrons. However, PEDOT: PSS is susceptible to moisture and oxygen of the air, causes interface instability through ITO and permeates into the active layer, erosion the ITO finally, the top low work-function (Al) is also particularly susceptible to oxidize in the air, leading to poor durability under ambient environment. [9] Therefore, employing an inverted device which exists the propensity of more stable, has an edge in PCE. At the same time, finding out an appropriate ETL between the ITO and the active layer not only can improve the extraction of photogenerated charge carriers, but inhibit most charge recombination, thereby increasing the PCE of iPSCs. [9-10]. For this reason, kinds of ETLs tend to include conjugated polymers [11-13], transition metal oxides [14] and hybrid materials [15]. Therefore, solution-processed ZnO is applied as ETL, due to it shows low temperature processability and high mobility, low work function (WF), high transparency and offers a convenience, simple device fabrication method [14-20]. However, many defects on the surface of ZnO nanoparticles prepared by sol-gel method are unavoidable, leading to the recombination of electron-hole pairs [18]. Internal doping of ZnO nanoparticles is better choice, both restraining surface charge recombination and improving electron extraction. And CdO nanoparticles possess higher conductivity and carrier mobility, which is result of intrinsic drawback of oxygen vacancies and cadmium [20]. And it also has a higher transparency within the scope of visible among the diverse metal oxide nanoparticles [19-21], thus comprehensively select cadmium-doped ZnO (termed hereafter CZO) by mole ratio as a fantastic ETL in solar cell applications is well option.

In view of previous discussion and research, we demonstrated a study based on a structure of inverted device is ITO/ETL/active layer/HTL/metal cathode in this paper, the Cd-doped ZnO nanoparticles of different concentrations (2.5%, 5%, 10%) by a facile wet chemistry synthetic protocol as ETL. The internal doping of metal ions in ZnO is a method, which can effectively reduce surface charge recombination and improve electron extraction. And 5% molar ratio (named after 5%) CZO can achieve the short-circuit current (J_{sc}) of from 16.30 mA/cm² to 17.15 mA/cm², the fill factor (FF) from 64.45% to 69.38%, power conversion efficiency (PCE) from 8.09% to 9.28%. Which significantly improves performance to supersede only ZnO nanoparticles. Meanwhile, the morphology of the ETL were characterized by atomic force microscopy (AFM), photo-electrochemical impedance spectroscopy (EIS), transmittance, the space charge limited current (SCLC), the charge dissociation probabilities ($P(E,T)$), which indicate that CZO can obviously improve transparency and morphology, and enhance conductivity. Therefore, the solution-processed of CZO nanoparticles, plays a momentous role in interfacial materials in PSCs or other devices domains requiring HTLs and paves the way for this material to be used in other optoelectronic and photovoltaic applications and beyond [20-26].

2. Experimental Section

2.1 Organic synthesis: Cd-Doped ZnO (CZO)

In simple terms, the synthesis process of doping disparate mole ratio (2.5%,5%,10%) Cd into ZnO nanoparticles was performed with a reasonable method. It's made of zinc acetate dihydrate ($Zn (Ac)_2 \cdot 2H_2O$, 0.0042mol) and cadmium acetate dihydrate ($Cd (Ac)_2 \cdot 2H_2O$, 0.0042mol) and then added into methanol (42mL) in a three-necked, round-bottomed flask. With these two reactants dissolved and mixed completely. Dissolving in potassium hydroxide (KOH, 0.0042mol) of methanol alcohol (CH_3OH , 20ml) was placed into the ongoing reaction within 5min, dropwise. The reaction mixtures were slowly stirred without pause 4 hours at 70°C roughly. Next, the solution washed twice with methanol followed by centrifugation. Which was dispersed in chloroform of appropriate volume, in the end, the solution was

diluted with n-butanol ($\text{CH}_3\text{CH}_2\text{CH}_2\text{CH}_2\text{OH}$) to 20mg/ml and ZnO nanoparticles were obtained [27].

2.2 Device Fabrication

PTB7-Th and PC₇₁BM were obtained from Calos and Sigma-Aldrich, respectively. Zinc acetate dihydrate ($\text{Zn}(\text{Ac})_2 \cdot 2\text{H}_2\text{O}$, 0.0042mol) and cadmium acetate dihydrate ($\text{Cd}(\text{Ac})_2 \cdot 2\text{H}_2\text{O}$, 0.0042mol) were purchased from Alfa Aesar, J&K Chemical Ltd., respectively, in the meanwhile, the method of device fabrication and characterization are same as this paper [27]. Measurements of AFM, EIS, ($P(E, T)$) are same as this paper [28].

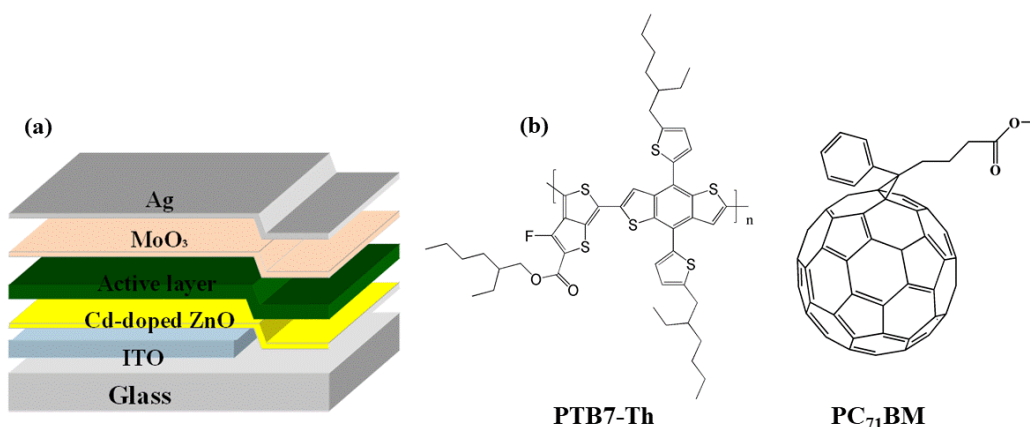


Figure 1. (a) the structure of device of iPSCs. (b) Chemical material structure of PTB7-Th and PC₇₁BM.

3. Results and Discussion

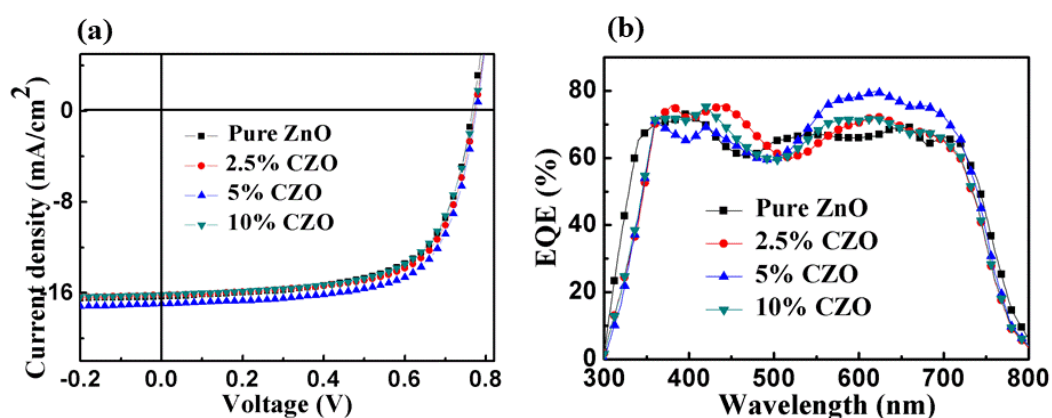


Fig. 2. (a) The J - V . (b) EQE curves of pure ZnO and various concentrations CZO as ETL under 100 mW/cm² simulated solar irradiation.

Table. 1. Performance parameters of inverted structure of various CZO as the ETL

ETL	V_{OC} (V)	J_{SC} (mA/cm ²)	FF (%)	PCE (%)	R_S ($\Omega \cdot \text{cm}^2$)	R_{Sh} ($\Omega \cdot \text{cm}^2$)
Pure ZnO	0.77	16.30	64.45	8.09%	3.93	854.93
2.5% CZO	0.77	16.19	66.66	8.31%	4.38	1078.75
5% CZO	0.78	17.15	69.38	9.28%	4.06	2702.70
10% CZO	0.77	16.12	64.85	8.05%	4.73	883.86

^a Averaged values of 10 devices.

To research the effects of CZO ETLs on iPSCs. Fig.1. shows the structure of inverted device, active materials. Both J–V characteristics of diverse concentrations CZO of iPSCs in Fig.2. (a) and Table1 show the device performance, 5% CZO has comparatively high parameter, yielding PCE of 8.86%, V_{OC} of 0.78V, J_{SC} of 16.95 mA/cm², FF of 67.03%. However, the inferior performances of devices have connection with smaller series resistance (R_S , 4.28 $\Omega \cdot \text{cm}^2$) and larger shunt resistance (R_{SH} , 1257.92 $\Omega \cdot \text{cm}^2$) of solar cell, which are able to reduce the injection barrier and the charge recombination rate. [29] It is worth mentioning that in this paper, the ETL of 5% CZO carries the highest PCE of PSCs, which can give rise to electron transport and extraction effectively.

The EQE spectrum Fig. 2(b). more hints that 5% CZO dominantly appeared at the extent of 550–750nm, where active layer has a distinct strong absorption, while the peak of the solar spectrum is coincidentally around 600 nm, which is beneficial to get sunlight and resulting in a higher J_{SC} in PSCs. Therefore, the higher EQE values of the device with a 5% CZO in the absorption region affirm that it more efficiently extracts tons of electrons from active layer, thus successfully reduces the recombination of carriers between the CZO of 5% content and the active layer.

In order to elucidate the peculiarity of exciton dissociation and charge collection, using the relationship between photocurrent density (J_{ph}) and effective voltage (V_{eff}), $J_{ph} = J_L - J_D$, J_D and J_L stand for the current density in darkness and illumination, respectively. And effective voltage ($V_{eff} = V_0 - V_{app}$), V_0 is the voltage ($J_{ph} = 0$), and V_{app} represents the applied voltage [28-30]. Fig. 3 (a) shows that J_{ph} increased with

V_{eff} in the low effective voltage range, indicating that the photocarriers dissociate into free charges, which are eventually collected at their respective electrodes [30]. Since the more efficient carrier transport directly causes increase in J_{sat} , the maximum exciton generation rate (G_{max}) is calculated by the formula $J_{\text{sat}} = qLG_{\text{max}}$, J_{sat} is the saturated photocurrent, q is the basic charge, and L is the activity layer thickness (100nm) [30]. Table 2 shows that a remarkable enhancement in G_{max} occurs after incorporating 5% Cd into the ETL of device, from the device with pure ZnO $1.10 \times 10^{28} \text{ m}^{-3} \cdot \text{s}^{-1}$ ($J_{\text{sat}} = 17.61 \text{ mA/cm}^2$) to the best performance $1.16 \times 10^{28} \text{ m}^{-3} \cdot \text{s}^{-1}$ ($J_{\text{sat}} = 18.57 \text{ mA/cm}^2$) with 5% Cd. Since the value of G_{max} shows the maximum number of photons absorbed. Therefore, the 5% CZO achieves a saturated region (18.57 mA/cm^2) among the devices, almost all of photoinduced holes and electrons are transported into the individual electrodes, and the probability of generating recombination becomes very small. Generally speaking, for iPSCs, the excitons generated by light are only partially dissociated into free carriers, $J_{\text{ph}}/J_{\text{sat}}$ could estimate the $(P(E,T))$, under short-circuit circumstance, which is presented in Figure 3 (b), the values of the pure ZnO and other three different concentration CZO ETL in devices are 93.27%, 94.66%, 96.29%, 96.40%, respectively. We corroborate from the description above that the trend of 5% Cd into ETL tend to cause highly efficient excitons dissociation and charges collection.

To verify the exist of CZO improving the device performance, therefore, Fig. 3 (c) shows under AM 1.5G 1000 W/m^2 irradiation (ITO/ZnO with Cd or without Cd/Al), the I-V data for these devices further show the 5% CZO-based device obviously exerts higher photo-generated conductivity than the basic of pure ZnO devices, producing high photoconductivity in favor of the photoinduced electron transfers from active layer to ETL. Therefore, major photo-conduct is to the benefit of restraining charge recombination and prompting electron to extract in PSCs. Thus, it is important for improving conductivity to restrain interfacial charges recombination and enhance charges extraction, electron/hole-transporting ability [32-33].

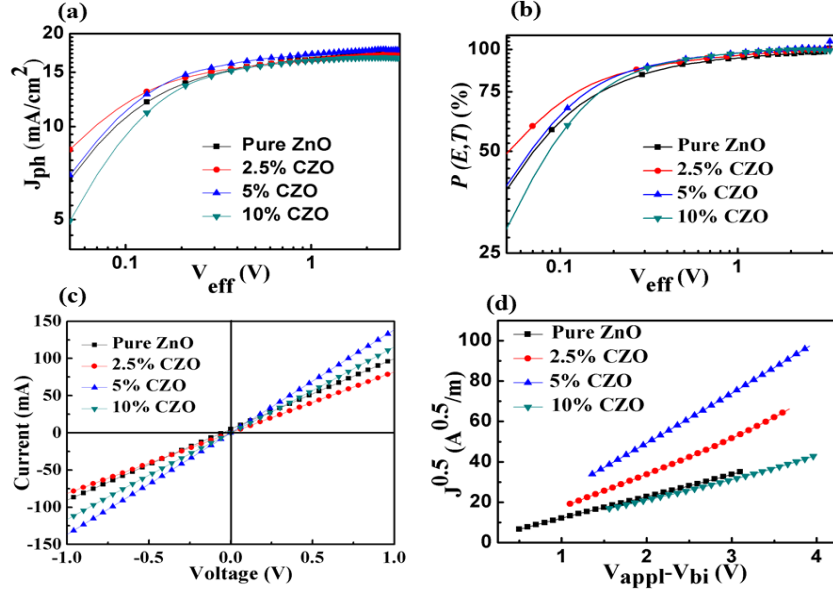


Figure 3. (a) The J_{ph} vs V_{eff} . (b) $P(E,T)$ vs V_{eff} . (c) I - V curves of the electron-only devices in the dark. (d) Electron mobility of ETL with different concentration CZO.

Table 2. G_{max} and corresponding J_{ph} / J_{sat} values of various Cd-doped concentrations (molar ratio)

ETL	$P(E, T)$	$G_{max}(m^{-3} \cdot s^{-1})$
Pure ZnO	93.27%	1.10×10^{28}
Cd-doped 2.5%	94.66%	1.07×10^{28}
Cd-doped 5%	96.29%	1.16×10^{28}
Cd-doped 10%	96.40%	1.04×10^{28}

The following discussion further confirms that CZO acts as ETL, accounting for the theory of FF enhancement in doped system. The J - V curves of electron-only (μ_e) devices along with individual Cd-doped ratios are shown in Fig (d), we elucidate the carrier mobilities of ETL by adopting the space-charge limited current (SCLC) model[33-37]. Electron-only devices were manufactured (ITO/CZO/PTB7-Th:PC₇₁BM/PDINO/Al). The electron mobility of the electron-only device takes advantage of the Mott-Gurney law. Which is described as:

$$J = \frac{9}{8} \epsilon_0 \epsilon_r \mu \frac{(V_{appl} - V_{bi})^2}{L^3}$$

J_D is the current density, ϵ_0 is the permittivity of free space (8.85×10^{-12} F/m), ϵ_r is the relative permittivity of the material (≈ 3.00), μ_e and V are the zero-field mobility, the effective voltage, respectively. L is the thickness of the active layer (100nm).

In the original device, the average electron mobility is calculated to be $8.33 \times 10^{-5} \text{ cm}^2 \cdot \text{v}^{-1} \cdot \text{s}^{-1}$. Duing to the electron mobility decreases gradually, 2.5% CZO ($1.49 \times 10^{-4} \text{ cm}^2 \cdot \text{v}^{-1} \cdot \text{s}^{-1}$), 5% CZO ($2.86 \times 10^{-4} \text{ cm}^2 \cdot \text{v}^{-1} \cdot \text{s}^{-1}$), 10% CZO ($5.31 \times 10^{-5} \text{ cm}^2 \cdot \text{v}^{-1} \cdot \text{s}^{-1}$), so photogenerated carriers loss are relatively low, which are able to well shed light on the enhancement FF. Therefore, the electron mobility increases and improves conductivity significantly, achieving high performance polymer solar cells in binary systems.

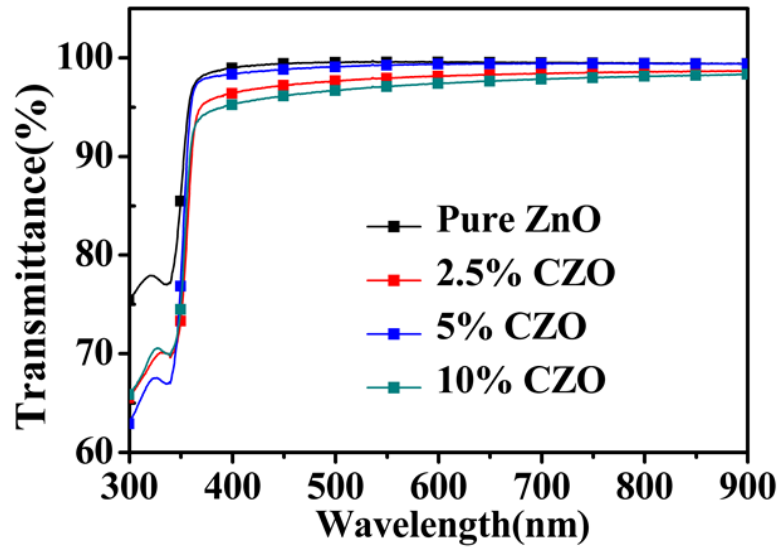


Figure. 4. Transmittance spectra of ETL under Cd-doped different concentration.

Through transmittance of the ETL investigated by UV-Vis spectroscopy, we measured the transmission characteristic of the ETLs, carrying different concentrations CZO in Fig. 4. The pure ZnO as a sample, prompting us to discover all the CZO films show quite fine light transmittance, making sure the high absorption and photocurrent generation. Particularly in the scope of 600-800 nm, it evidently implicates that 5% CZO ETL can be perfectly used as an interface modification layer of ITO glass. Therefore, the visible light can effectively transport from the active layer to ITO/ETL the with little apparent absorption loss.

In order to further evaluate the essential impact of the ETL properties between electrode and active layer on device performance. As shown in Fig.5. Atomic force microscopy (AFM) studies indicate that the root-mean-square (RMS) surface roughness of the pure ZnO and CZO film decreases from 3.08 to 2.12 nm ((a)-(b)).

Although the surface morphology of all CZO look alike but the roughness of 5% is the smallest, which means properly 5% CZO might higher improve the contact at the CZO/active blend. Thus, we believe that smoother surfaces of these films are consistent with higher FF, which facilitate uniform, intimate contact with the PTB7-Th: PC₇₁BM photoactive layer. Therefore, with 5% CZO nanocomposite thin films as an ETL regards as a better select compared with only ZnO devices, and achieving high performance polymer solar cells.

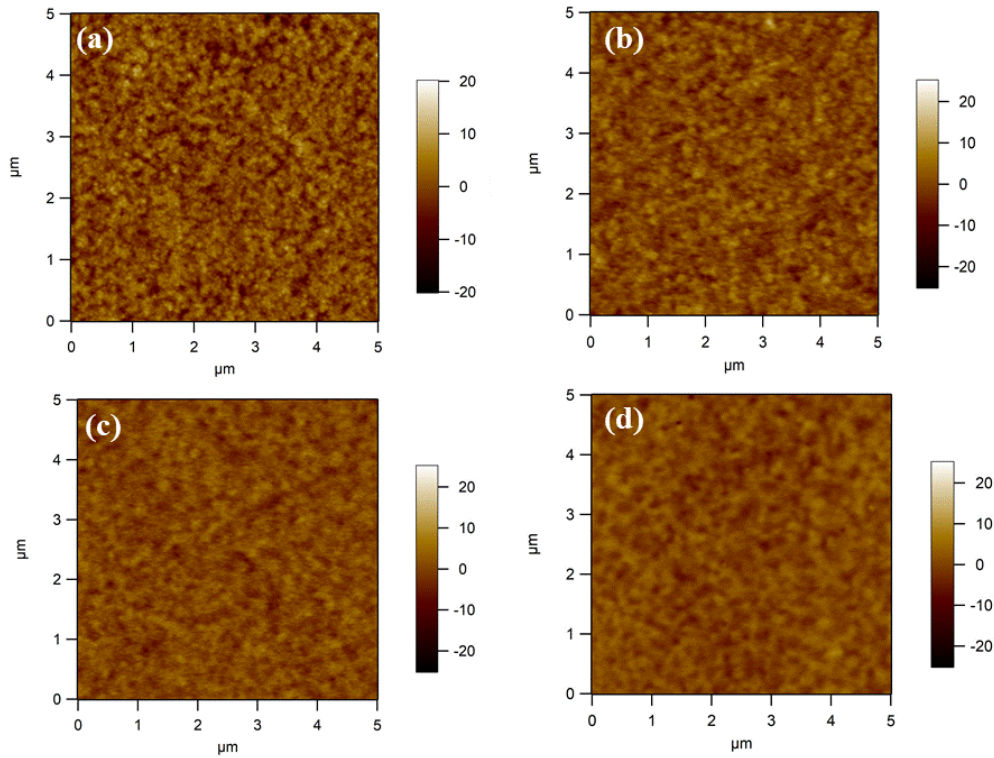


Fig. 5. AFM phase images of the ETL with different Cd concentration (a) ZnO (b) 2.5% (c) 5% (d) 10%. (5×5 um scan size)

We further investigate the dynamics of carrier transport through the photoelectron (EIS). Which confirms the interfacial charge extraction and recombination on the interface between the active layer and ETL. The equivalent circuit includes a resistance R_s in series with a resistance R_1 and a constant phase element (CPE) in parallel. R_s , R_1 represent resistive losses, photoactive layer resistance in this equivalent circuit, respectively. the CPE indicates non-uniform interface causes a non-ideal capacitor. CPE, including CPE-T and CPE-P two parameters. CPE-T represents a value of capacitance and CPE-P is a factor relative to an ideal capacitor.

When CPE-P is equal to 1, the CPE is considered to be an ideal capacitor without defects and/or grain boundaries. In Fig. 6. shows the Nyquist plot of the devices with and without Cd-doped buffer layer, which was measured in dark condition, 5% CZO ETL significantly lower than other devices, indicating more efficient electron extraction and reducing interfacial charge recombination at interface [38-42].

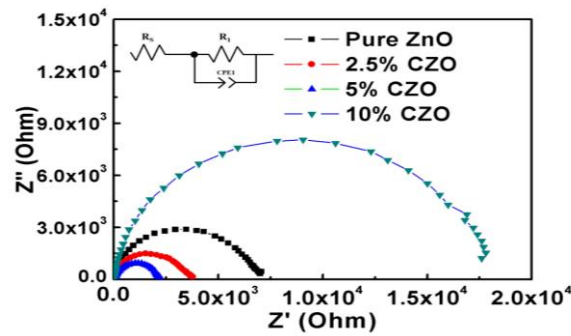


Fig. 6. Nyquist plot of the PSCs with pure ZnO and different Cd-doped concentration

4. Conclusions

In summary, the electron transport layers of different concentrations CZO were characterized by AFM, SCLC, transmittance, $P(E,T)$, EIS etc. The experimental and theoretical results show strategy that CZO of various concentration can supersede only ZnO as ETL, Therefore, synthesized CZO as ETL has many advantages, such as high photovoltaic performance, simple and low-temperature (70°C) solution-processed, especially 5% concentration, which not only provides a PCE of 9.28%, but optimizes solar cell performance, improve conductivity and have relatively high optical transmittance of thin films contributing to enhance photovoltaic performance. And it will be a potential interface material for transport layer in future PSCs.

Acknowledgments

The authors thank the National Natural Science Foundation of China (no. 51602139), the Natural Science Foundation of Gansu Province (no. 18JR3RA108), Excellent Team of Scientific Research (201705) and the Foundation of A Hundred Youth Talents Training.

Conflicts of interest

There are no conflicts of interest to declare

References:

1. Gao, K.; Li, L. S.; Lai, T. Q.; Xiao, L. G.; Huang, Y.; Huang, F.; Peng, J. B.; Cao, Y.; Liu, F.; Russell, T. P.; Janssen, R. A. J.; Peng, X. B. *Journal of the American Chemical Society*. **2015**, 137, 7282-7285. doi: 10.1021/jacs.5b03740
2. Liu, T.; Gao, W.; Zhang, G. Y.; Zhang, L.; Xin, J. M.; Ma, W.; Yang, C. L.; Yan, H.; Zhan, C. L.; Yao, J. N. *Sol RRL*. **2019**, 3, 1800376. doi: 10.1002/solr.201800376
3. Liu, T.; Meng, D.; Cai, Y. H.; Sun, X. B.; Li, Y.; Huo, L. J.; Liu, F.; Wang, Z. H.; Russell, T. P.; Sun, Y. M. *Adv Sci*. **2016**, 3, 1600117. doi: 10.1002/advs.201600117
4. Liu, T.; Huo, L.; Chandrabose, S.; Chen, K.; Han, G.; Qi, F.; Sun, Y. *Adv Mater*. **2018**, 30, 1707353. doi: 10.1002/adma.201707353
5. Gao, K.; Miao, J. S.; Xiao, L. G.; Deng, W. Y.; Kan, Y. Y.; Liang, T. X.; Wang, C.; Huang, F.; Peng, J. B.; Cao, Y.; Liu, F.; Russell, T. P.; Wu, H. B.; Peng, X. B. *Adv Mater*. **2016**, 28, 4727–4733. doi: 10.1002/adma.201505645
6. Li, J. F.; Liang, Z. Z.; Peng, Y. C.; Lv, J.; Ma, X. Y.; Wang, Y. F.; Xia, Y. J. *Polymers*. **2018**, 10, 703. doi: 10.3390/polym10070703
7. Liang, Z. Z.; Tong, J. F.; Li, H. D.; Wang, Y. F.; Wang, N. N.; Li, J. F.; Yang, C. Y.; Xia, Y. J. *J Mater Chem A*. **2019**, 7, 15841–15850. doi: 10.1039/C9TA04286E
8. Li, G.; Zhu, R.; Yang, Y.; *Nat Photon*. **2012**, 6, 153–161. doi: 10.1038/nphoton.2012.11
9. Wang, J. T.; Zhang, J.; Meng, B.; Zhang, B. H.; Xie, Z. Y.; Wang, L. X. *ACS Appl Mater Interfaces*. **2015**, 7, 13590–13596. doi: 10.1021/acsami.5b02997
10. Du, Z. K.; Bao, X. C.; Li, Y. H.; Liu, D. Y.; Wang, J. X.; Yang, C. M.; Wimmer R.; Städe, L. W.; Yang, R. Q.; Yu, D. H.; *Advanced Energy Materials*. **2017**, 8, 1701471. doi:10.1002/aenm.201701471
11. Zhao, W. C.; Qian, D. P.; Zhang, S. Q.; Li, S. S.; Inganäs, O.; Gao, F.; Hou, J. H. *Adv Mater*. **2016**, 28, 4734–4739. doi: 10.1002/adma.201600281
12. Page, Z. A.; Liu, Y.; Duzhko, V. V.; Russell, T. P.; Emrick, T. *Science*, **2014**, 346, 441–444. doi: 10.1126/science.1255826
13. Bao, X. C.; Zhang, Y. C.; Wang, J. Y.; Zhu, D. Q.; Yang, C. P.; Li, Y. H.; Yang, C. M.; Xu, J. T.; Yang, R. Q.; *Chemistry of Materials*. **2017**, 16, 6766–6771. doi:10.1021/acs.chemmater.7b01650
14. Zhang, J.; Wang, J. T.; Fu, Y. Y.; Zhang, B. H.; Xie, Z. Y. *J Mater Chem C*. **2014**, 2, 8295–8302. doi: 10.1039/C4TC01302F
15. Huang L, Chen L, Huang P, Wu, F.; Tan, L.; Xiao, S.; Zhong, W.; Sun, L.; Chen, Y. **2016**, 24, 4852-4860. *Adv Mater*. **2016**, 28:4852–4860

16. Rehman, F.; Mahmood, K.; Khalid, A.; Zafar, M. S.; Hameed, M. *Journal of Colloid and Interface Science*. **2019**, 535, 353–362. doi: 10.1016/j.jcis.2018.10.011
17. Steigera, P.; Zhang, J.; Harrabi, K. Hussein, I. A.; Downing, J. M.; McLachlan, M. A. *Thin Solids Films*, **2018**, 645,417–423. doi: 10.1016/j.tsf.2017.11.021
18. Richardson, B. J.; Wang, X. Z.; Almutairia, A.; Yu, Q. M. *J Mater Chem A*, **2015**, 3, 5563–5571. doi: 10.1039/C5TA00400D
19. Yang, Z. Y.; Zhang, T.; Li, J. Y.; Xue, W.; Han, C. F.; Cheng, Y. Y.; Qian, L.; Cao, W. R.; Yang, Y. X.; Chen, S. *Sci Rep*, **2017**, 7, 9571. doi: 10.1038/s41598-017-08613-7
20. Moon, B. J.; Lee, K. S.; Park, S, Y.; Kim, S. H.; Shim, J.; Bae, S. K.; Park, M.; Lee, Chang-L.; Choi, W. K.; Yi, Y. J.; Hwang, J. Y.; Son, D. H. *Nano Energy*.**2016**, 20, 221–232. doi: 10.1016/j.nanoen.2015.11.039
21. Aksoy S, Caglar Y, Ilican S, Caglar M. *international journal of hydrogen energy* **2009**, 34, 5191–5195. doi: 10.9790/4861-0805010105
22. Lin, Z. H.; Chang, J. J.; Zhang, C. F.; Zhang , J. S.; Wu, J. S.; Hao, Y. *J Mater Chem C*. **2016**, 4, 6169-6175. doi: 10.1039/C6TC00760K
23. Yakuphanoglu, F.; Ilican, I.; Caglar, M.; Caglar, Y. *Superlattices and Microstructures*, **2010**, 47, 732–743. doi: 10.1016/j.spmi.2010.02.006
24. Fouzri, A.; Boukadhaba, M. A.; Oumezzine, M.; Sallet, V. *Thin Solid Films*, **2012**, 520, 2582–2588. doi: 10.1016/j.tsf.2011.11.027
25. Liu, J. Z.; Yan, P. X.; Yue, G. H.; Chang, J. B.; Zhuo, R. F.; Qu, D. M. *Mater Lett*, **2006**, 60, 3122–3125. doi: 10.1016/j.matlet.2006.02.056
26. Zheng, B.; Lian, J.; Zhao, L.; Jing, Q. *Appl Surf Sci*, **2011**, 257, 5657–5662. doi: 10.1016/j.apsusc.2011.01.070
27. Lupan, O.; Pauporté, T.; Bahers, T. L.; Ciofini, L.; Viana, B. *J Phys Chem C*, **2011**, 115, 14548–14558. doi: 10.1021/jp202608e
28. Yang, F.; Xu, Y.; Gu, M.; Zhou, S.; Wang, Y.; Lu, K.; Liu, Z.; Ling, X.; Zhu, Z.; Chen, J.; Wu, Z.; Zhang, Y.; Xue, Y.; Li, F.; Yuan, J.; Ma, W. *Journal of Materials Chemistry A*, **2018** 00, 1-3. doi: 10.1039/C8TA05946B
29. Chen, W. C.; Huang, G. Y.; Li, X. M.; Wang, H.; Li, Y. H.; Jiang, H. X.; Zheng, N.; Yang, R. Q. *ACS Appl Mater Interfaces*, 2018, 10, 42747–42755. doi: 10.1021/acsami.8b16554
30. Han, L. L.; Uranbileg, N.; Jiang, S. S.; Xie, Y.; Jiang H. X.; Lan, Z. G.; Yu, D. H.; Bao, X. C.; Yang, R. Q. *Journal of Materials Chemistry A*, **2012**, 00, 1-3. doi: 10.1039/x0xx00000x

31. Li, J. F.; Wang, Y. F.; Liang, Z. Z.; Wang, N. N.; Tong, J. F.; Yang, C. Y.; Bao, X. C.; Xia, Y. J. *ACS Appl Mater*, **2019**, 11, 7022–7029. doi: 10.1021/acsami.8b20466
32. Li, J. F.; Liang, Z. Z.; Wang, Y. F.; Li, H.; Tong, J. F.; Bao, X. C.; Xia, Y. J. *J Mater Chem C* **2018**, 6, 11015–11022. doi: 10.1039/C8TC03612H
33. Zhou, M.; Sun, Q. J.; Gao, L. Y.; Wu, J.; Zhou, S. L.; Li, Z. F.; Hao, Y. Y.; Shi, F. *Organic Electronics*, **2016**, 32, 34–40 doi: 10.1016/j.orgel.2016.02.003
34. Wang, J. T.; Yan, C.; Zhang, X. Q.; Zhao, X. F.; Fu, Y. Y.; Zhang, B. H.; Xie, Z. Y. *Journal of Materials Chemistry C*, **2016**, 46, 10820–10826. doi: 10.1039/C6TC04366F
35. MbuleT, P. S.; KimbB. S.; SwartaO. C.; Ntwaeaborwa, M. *Solar Energy Materials and Solar Cells*, **2013**, 112, 6–12. doi: 10.1016/j.solmat.2013.01.010
36. Shrotriya, V.; Yao, Y.; Li, G.; Yang, Y. *Applied Physics Letters*, **2006**, 6, 063505. doi: 10.1063/1.2335377
37. Li, X. M.; Huang, G. Y.; Zheng, N.; Li, Y. H.; K, X.; Qiao, S. L.; Jiang, H. X.; Chen, W. C.; Yang, R. Q. *Sol RRL*, **2019**, 3, 1900005. doi: 10.1002/solr.201900005
38. He, Z. C.; Zhong, C. M.; Huang, X.; Wang, W-Yeung.; Wu, H. B.; Chen, L. W.; Su, S. J.; Cao, Y. *Adv Mater*, **2011**, 23, 4636–4643. doi: 10.1002/adma.201103006
39. Wang, X. C.; Du, Z. R.; Dou, K. K.; Jiang, H. X.; Gao, C. L.; Han, L. L.; Yang, R. Q. *Adv Energy Mater*. **2018**, 1, 1802530. doi: 10.1002/aenm.201802530
40. Liu, T.; Luo, Z. H.; Fan, Q. P.; Zhang, G. Y.; Zhang, L.; Gao, W.; Guo, X.; Ma, W.; Zhang, M. J.; Yang, C. L.; Li, Y. F.; Yan, H. *Energy & Environmental Science*, **2018**, 11, 3275-3282. doi: 10.1039/C8EE01700J
41. Li, J. F.; Lv, J.; Peng, Y. C.; Cao, X. D.; Tong, J. F.; Xia, Y. J. *Polym Adv Technol*, **2018**, 29, 2237–2244. doi: 10.1002/pat.4334
42. Borse, K.; Sharma, R.; Gupta, D.; Yella, A. *RSC Adv*. **2018**, 8, 5984–5991. doi: 10.1039/c7ra13428b
43. Zheng, Y. F.; Goh, T.; Fan, P. F.; Shi, W.; Yu, J. S.; Taylor, A, D. *ACS Appl Mater Interface*, **2016**, 24, 15724-15731. doi: 10.1021/acsami.6b03453